

# Accuracy Evaluation Trial of Mixed Reality-Guided Spinal Puncture Technology

Jiajun Wu<sup>1,2,\*</sup>, Lei Gao<sup>1,2,\*</sup>, Qiao Shi<sup>3</sup>, Chunhui Qin<sup>4</sup>, Kai Xu<sup>1,2</sup>, Zhaoshun Jiang<sup>1,2</sup>, Xixue Zhang<sup>1,2</sup>, Ming Li<sup>5</sup>, Jianjian Qiu<sup>6,\*</sup>, Weidong Gu<sup>1,2,\*</sup>

<sup>1</sup>Department of Anesthesiology, Huadong Hospital Affiliated to Fudan University, Shanghai, 200040, People's Republic of China; <sup>2</sup>Shanghai Key Laboratory of Clinical Geriatric Medicine, Shanghai, 200040, People's Republic of China; <sup>3</sup>Department of Anesthesiology, International Peace Maternity and Child Health Hospital of China, School of Medicine, Shanghai Jiao Tong University, Shanghai, 200030, People's Republic of China; <sup>4</sup>Department of Pain Management, Yueyang Integrated Traditional Chinese Medicine and Western Medicine Hospital Affiliated to Shanghai University of Traditional Chinese Medicine, Shanghai, 200437, People's Republic of China; <sup>5</sup>Department of Radiology, Huadong Hospital affiliated to Fudan University, Shanghai, 200040, People's Republic of China; <sup>6</sup>Department of Radiation Oncology, Huadong Hospital Affiliated to Fudan University, Shanghai, 200040, People's Republic of China

\*These authors contributed equally to this work

Correspondence: Weidong Gu; Jianjian Qiu, Email hdmz0800@163.com; qiujianjian@fudan.edu.cn

**Purpose:** To evaluate the accuracy of mixed reality (MR)-guided visualization technology for spinal puncture (MRSp).

**Methods:** MRSp involved the following three steps: 1. Lumbar spine computed tomography (CT) data were obtained to reconstruct virtual 3D images, which were imported into a HoloLens (2nd gen). 2. The patented MR system quickly recognized the spatial orientation and superimposed the virtual image over the real spine in the HoloLens. 3. The operator performed the spinal puncture with structural information provided by the virtual image. A posture fixation cushion was used to keep the subjects' lateral decubitus position consistent. 12 subjects were recruited to verify the setup error and the registration error. The setup error was calculated using the first two CT scans and measuring the displacement of two location markers. The projection points of the upper edge of the L3 spinous process (L3↑), the lower edge of the L3 spinous process (L3↓), and the lower edge of the L4 spinous process (L4↓) in the virtual image were positioned and marked on the skin as the registration markers. A third CT scan was performed to determine the registration error by measuring the displacement between the three registration markers and the corresponding real spinous process edges.

**Results:** The setup errors in the position of the cranial location marker between CT scans along the left-right (LR), anterior-posterior (AP), and superior-inferior (SI) axes of the CT bed measured  $0.09 \pm 0.06$  cm,  $0.30 \pm 0.28$  cm, and  $0.22 \pm 0.12$  cm, respectively, while those of the position of the caudal location marker measured  $0.08 \pm 0.06$  cm,  $0.29 \pm 0.18$  cm, and  $0.18 \pm 0.10$  cm, respectively. The registration errors between the three registration markers and the subject's real L3↑, L3↓, and L4↓ were  $0.11 \pm 0.09$  cm,  $0.15 \pm 0.13$  cm, and  $0.13 \pm 0.10$  cm, respectively, in the SI direction.

**Conclusion:** This MR-guided visualization technology for spinal puncture can accurately and quickly superimpose the reconstructed 3D CT images over a real human spine.

**Keywords:** mixed reality, spinal puncture, immobilization, superimposition, setup error, registration error

## Introduction

With the increasing adoption of enhanced recovery after surgery (ERAS) protocols, spinal anesthesia plays an important role in reducing patients' cardiovascular complications, improving postoperative analgesia, and accelerating the process of postoperative rehabilitation.<sup>1-10</sup> Conventional spinal puncture, which is a "blind technique", is performed by manual palpation using Tuffier's line (the horizontal line connecting the superior iliac crests) as a surface landmark.<sup>11,12</sup> However, in elderly patients with degenerative spondylopathy, the difficulty of puncture is greatly increased, which reduces the success rate of puncture and increases the risk of related complications such as nerve injury. Recently, visualization techniques, such as X-ray-guided and ultrasound-guided spinal puncture techniques, have been developed in clinical anesthesia. However, both X-ray- and ultrasound-guided spinal puncture techniques have certain limitations that restrict their widespread use.<sup>13,14</sup> X-ray-guided spinal puncture is

generally used only for patients in the prone position, while spinal anesthesia puncture requires the patient to be in the lateral decubitus or sitting position. Ultrasound-guided spinal puncture with a handheld ultrasound probe is inconvenient for spinal puncture in clinical practice. Hence, it is very important to find a visualization technology to meet the need for spinal puncture guidance.

With the development of artificial intelligence technology, mixed reality (MR) has gradually been adopted as a new visualization technology in many medical fields, including clinical diagnosis, medical education, and intraoperative navigation.<sup>15</sup> MR is a blend of the physical and digital worlds, unlocking natural and intuitive 3D interactions among humans, computers, and the environment, presenting both the real world and the virtual world in one display.<sup>16</sup> The patient's preoperative CT images are converted into a virtual 3D image. When the user wears the MR headset, the virtual image is presented at a 1:1 scale on the actual anatomical location of the corresponding body structures. Thus, the MR system provides the operator with the equivalent of a fluoroscopic view during the procedure. The operator can proceed with the spinal puncture with both hands-free, and the patient can maintain the standard lateral decubitus position for spinal puncture. If MR technology can guide spinal puncture, this application will be of great significance for improving the success rate and accuracy of puncture. To date, however, the use of MR in guiding spinal punctures in humans has not been reported.

This study aimed to evaluate the accuracy of MR-guided spinal puncture (MRsp), an MR-guided visualization technology for spinal puncture. MRsp consists of three parts: virtual 3D image reconstruction, automatic adaptation of the virtual image over the real spine and spinal puncture with structural information provided by the virtual image. To evaluate the accuracy of MRsp, this study mainly focused on the consistency of the patient's lateral decubitus position at different times and the accuracy of the matching between the virtual image in MR and the real lumbar spine. The setup error and the registration error were measured.

## Materials and Methods

This study was approved by the Ethics Committee of Huadong Hospital affiliated with Fudan University (protocol code: 2023K015), and written informed consent was obtained from all subjects participating in the study. The study was registered before subject enrollment at [chictr.org.cn](https://www.chictr.org.cn) (ChiCTR2300068525; Principal investigator: Dr. Weidong Gu; <https://www.chictr.org.cn/showproj.aspx?proj=190253>; Date of registration: February 2023).

### MR Hardware

The 2nd gen HoloLens (Figure 1), a head-mounted MR display developed by Microsoft, was used in this study. In cooperation with Suzhou Reacool Medical Technology Co., Ltd., the self-designed Reacool medical MR (MMR) system was used to obtain the lumbar CT images of subjects. Then, the data were transformed into virtual 3D images of the lumbar spine (details in [CT Scanning and CT Simulation](#)). The virtual 3D images were uploaded into the HoloLens using 3D diffraction display technology, and images of the virtual objects were projected into the eyes at a specific angle and wavelength through two transparent light-guide lenses on the device, thus blending virtual images with light from the real environment to produce a full range of images.<sup>17</sup>

## Design of the In-House MRsp Technology

### CT Scanning and CT Simulation

While remaining in the lateral decubitus position with the arms wrapped around the knees, each subject underwent CT on a Siemens Somatom Definition AS R CT scanner (Siemens Somatom Sensation, Munich, Germany) with a pitch of 1.5, a slice thickness of 1 mm and a flat table for consistency. CT images of the lumbar spine in Digital Imaging and Communications in Medicine (DICOM) format were transformed into holographic lumbar spine images by the patented Reacool MMR system through four steps: stitching, stripping, surface reduction, and synthesis. The virtual 3D images were displayed and stored in the MMR system and viewed using the HoloLens.

### In-House Positioning and Immobilization Technique for Consistency

Inconsistency in the patient's position between the CT scan and the spinal puncture may lead to dislocation between the virtual image and the real lumbar spine, which may reduce the success rate of MRsp. Thus, a posture fixation cushion,



**Figure 1** HoloLens (2nd gen) hardware, Microsoft Corp., 2019.

modified from traditional body vacuum cushions for radiotherapy (Civco Medical Solutions; Kalona, Indiana, USA),<sup>18</sup> was optimized for immobilizing the patient in the lateral decubitus position (Figure 2). Filled with polyvinyl chloride particles ( $C_2H_3Cl$ )<sub>n</sub> ( $S\phi \approx 4$  mm), it becomes rigid when a vacuum is applied and helps the patient maintain a fundamentally consistent posture across multiple CT scans. Parts I, II, and III of the cushions, as marked in Figure 2, were used to immobilize the subject's scapulae, buttocks, and iliac waist, respectively, so that the subject was fixed in a lateral decubitus position with the arms wrapped around the knees (a standard position for spinal puncture). Six fixation belts (A, B, C, D, E, and F) were connected with the paired belts (A', B', C', D', E', and F') by tear-off buckles, and the lengths of all the paired belts were recorded and marked when the subject was placed in the lateral decubitus position for the first CT scan. The lengths were kept the same for the second scan to keep the subject in the same position.

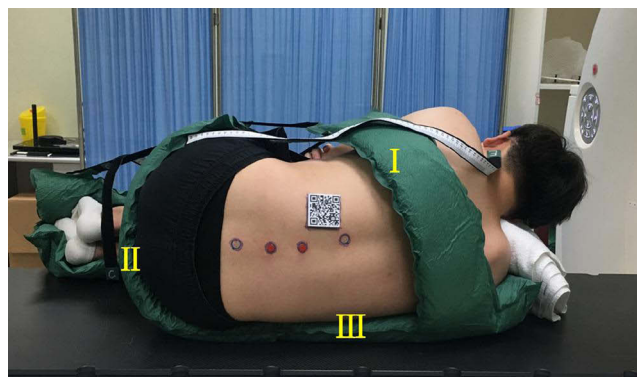


**Figure 2** In-house modified vacuum cushion for fixation in the lateral decubitus position.

## MR-Based Virtual 3D Models Automatically Adapted to Subjects' Spinal Anatomy

The operator wore the HoloLens when performing the spinal puncture. The MR glasses quickly (in approximately one second) recognized the spatial orientation and automatically superimposed the virtual image over the real lumbar spine by scanning a quick response code (QR code) (a in Figure 3) attached to the dorsal skin of the subject through eye-tracking technology. Two position markers, the beacons made from isotactic polypropylene (b/c in Figure 3), attached to the skin of the lumbar spine, served as location and reference markers for accurately matching the virtual image to the real lumbar spine. The operator manually fine-tuned the spatial positions of the virtual beacons (b'/c' in Figure 3) in four directions (yellow arrows in Figure 3) until they completely overlapped with the real beacons. This calibration ensured an accurate match between the virtual image and the real lumbar spine by adding a manual adjustment step to the automatic alignment step. With the image of the virtual spine overlaying the real body, the operator could proceed with the spinal puncture. This is the main procedure of MRsp.

## Methods and Workflow for Evaluation of the Setup Error and Registration Error of MRsp Technology

To verify the accuracy of MRsp, the displacement between the virtual spine image and the real spine was measured to determine whether it was within the acceptable range. Methods for evaluating the setup error and registration error of MRsp technology were designed. The workflow is shown in Figure 4.

12 volunteers with an average age of 19.5 years old (range, 18–24; standard deviation, 1.9) were enrolled in this trial from February 2023 to March 2023 (① in Figure 4). Those with a history of lumbar trauma, surgery, or malformation were excluded, and those who dropped out of the study were eliminated from the analysis.

The total procedure required three lumbar spine CT scans to be performed for each subject. The subjects were immobilized in the lateral decubitus position with a modified vacuum fixation cushion, and the lengths of the six fixation belts were recorded during the first CT scan (② and ③ in Figure 4). After standing up and leaving the CT bed for approximately 5–10 minutes (④ in Figure 4), the subject was refixed in the same position according to the recorded lengths of the belts and underwent the second CT scan (② and ③ in Figure 4). A commercial image registration and evaluation system with submillimeter system error (Eclipse® V13.5 software; Varian, USA) was used to calculate the displacement of the location markers (the beacons; Figure 3 left, b and c) between the two CT scans to evaluate the setup errors at the two positions in three dimensions, ie, in the left-right (LR), anterior-posterior (AP), and superior-inferior (SI) directions according to the direction of CT bed movement (⑤ in Figure 4).

The virtual 3D image was automatically adapted to the subject's real back by using MRsp technology (⑥ in Figure 4). Three registration markers (red spots, Figure 5 right) were placed on the subject's lumbodorsal skin according to the projection points of the upper edge of the L3 spinous process (L3↑), the lower edge of the L3 spinous process (L3↓), and the lower edge of the L4 spinous process (L4↓) in the virtual image (red spots, Figure 5 left) (⑦ in Figure 4). A third CT scan was performed (⑧ in

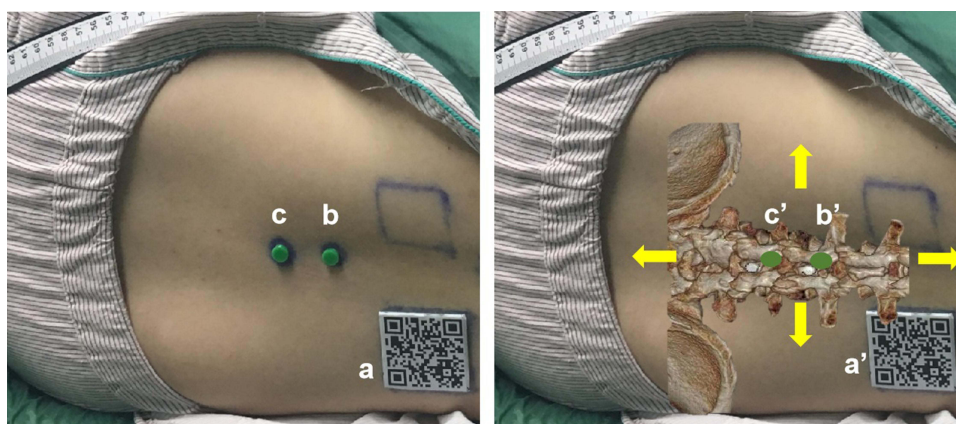


**Figure 3** MR-based virtual 3D models automatically adapted to one subject. Left: A subject in the lateral decubitus position with a QR code (a) and two beacons (b/c) affixed to the dorsal skin. Right: The position of the subject's virtual 3D lumbar model was automatically and manually adapted to match the real lumbar spine. b'/c': Virtual beacons. Yellow arrows: manual fine-tuning in four directions.

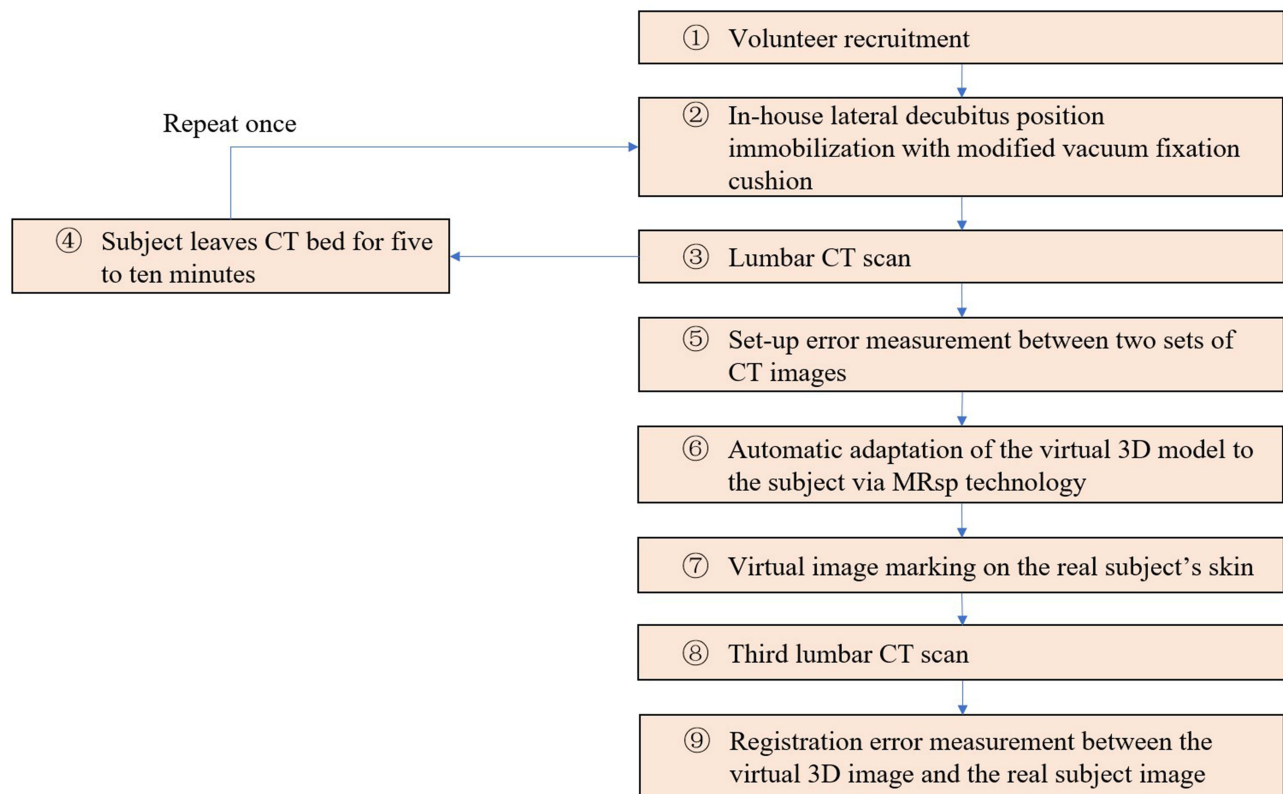


**Figure 4** Accuracy trial workflow for MRsp.

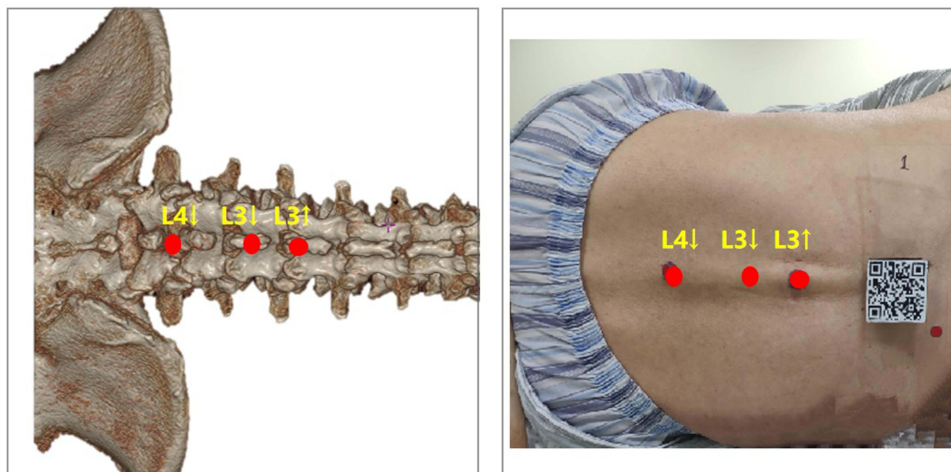


**Figure 5** Method of projecting the virtual image over the real spine. L3↑: Upper edge of the L3 spinous process. L3↓: Lower edge of the L3 spinous process. L4↓: Lower edge of the L4 spinous process.

**Figure 4**). By measuring the displacement between the three registration markers and the corresponding real spinous process edges in the third CT scan, the registration error was calculated (⑨ in **Figure 4**).

## Statistical Analysis

Data were analyzed using the statistical software package SPSS (version 24.0; IBM, Chicago, IL, USA). Continuous variables were tested for normality with the Kolmogorov–Smirnov test. Normally distributed variables are expressed as the mean  $\pm$  standard deviation, and nonnormally distributed variables are expressed as the median [interquartile range].

**Table 1** Setup Errors and Registration Errors of MRsp (n=12: Mean  $\pm$  Standard Deviation)

cm	Set-Up Error		Registration Error		
	Cranial Marker	Caudal Marker	L3 $\uparrow$	L3 $\downarrow$	L4 $\downarrow$
x-axis	0.09 $\pm$ 0.06	0.08 $\pm$ 0.06	N/A	N/A	N/A
y-axis	0.30 $\pm$ 0.28	0.29 $\pm$ 0.18	0.29 $\pm$ 0.17	0.38 $\pm$ 0.25	0.42 $\pm$ 0.35
z-axis	0.22 $\pm$ 0.12	0.18 $\pm$ 0.10	0.11 $\pm$ 0.09	0.15 $\pm$ 0.13	0.13 $\pm$ 0.10

**Notes:** The x-axis corresponds to the left-right (LR) direction of the CT bed. The y-axis corresponds to the anterior-posterior (AP) direction of the CT bed. The z-axis corresponds to the superior-inferior (SI) direction of the CT bed.

**Abbreviation:** N/A, not available.

## Results

The setup and registration errors in this study are listed in Table 1. The three-dimensional setup error was the smallest of the two error types (at  $< 3$  mm). However, the registration error was less than 4 mm and still within the clinically acceptable range. The setup error in the LR direction of the CT bed was minimized by using the modified posture fixation cushion.

The setup error was calculated according to the 3D CT images shown in Figure 6. The purple circle represented the position of the cranial position marker (b in Figure 3) during the first CT scan, while the white circle represented the position of the same beacon during the second CT scan. The precise overlap of the two circles in three dimensions indicated that there was little setup error between the two positions. The caudal position marker's displacement in three dimensions was measured in the same way.

The registration error was measured as shown in Figure 7. The purple circle represented the real L3 $\uparrow$ , while the white circle is the registration marker on the skin corresponding to the virtual image of L3 $\uparrow$ . The displacement measurements between the two points in the AP and SI directions of the bed were considered the registration error between the virtual image and the real spine. The L3 $\downarrow$  and L4 $\downarrow$  registration errors were measured in the same way.

## Discussion

Traditional techniques, such as X-ray and ultrasound, have been investigated for the visual guidance of spinal puncture. Tanaka et al<sup>19</sup> found that the accuracy of puncture point location by X-ray guidance (67%) was better than that of the traditional anatomic localization approach (29–59%). However, the X-ray-guided spinal puncture technique is generally used only for patients in the prone position, while spinal anesthesia puncture requires the patient to be in the lateral decubitus or sitting position. The operator must wear heavy radioprotective clothing, which is not feasible for performing clinical spinal anesthesia.

Li et al<sup>20</sup> found that ultrasound examination before puncture could facilitate spinal anesthesia in the lateral position in obese parturients by improving the first-attempt success rate, reducing the number of needle passes and puncture



**Figure 6** Measurement of setup error on the three major anatomical planes on 3D CT. The projections of the cranial beacon in the first CT (purple circle) and the second CT (white circle) were compared, and the 3D displacements were calculated (a: transverse plane; b: coronal plane; c: sagittal plane).



**Figure 7** Measurement of lumbar spine registration error on 3D CT. The displacement values between the real L3 (purple circle) and the virtual L3 registration marker (white circle) in the AP and SI directions of the bed were considered the registration error.

attempts, shortening the total procedure time, and improving patient satisfaction. However, ultrasound-guided spinal puncture with a handheld ultrasound probe is inconvenient in clinical practice. Moreover, the poor visualization of peri vertebral structures by ultrasound limits the widespread use of this technique.

In recent years, with the development of science and technology and the progress of medicine, MR technology has been gradually applied in several medical fields, such as diagnosis, surgery, rehabilitation treatment, education, and training.<sup>21–26</sup> Freschi et al found that MR could improve ultrasound probe manipulation training, with a success rate for visualizing the target structure of 78% in the hybrid group versus 45% in the physical group ( $P=0.04$ ).<sup>27</sup> Wang et al presented an augmented reality navigation system for dental surgery based on a 3D image overlay. They found that the mean overall error of the 3D image overlay was 0.71 mm, which met clinical needs.<sup>25</sup>

Recently, Sargsyan et al developed an augmented reality application to enhance training in the lumbar puncture procedure on a specially designed manikin of the lower back of the human body.<sup>26</sup> There were some differences between our study and theirs. First, for research objectives, Sargsyan et al used the manikin for study, while our research objective was the real human spine. The structure of the human spine is more complex and changeable than that of a model, and the superimposition between the virtual image and the real spine will be more difficult. In the present study, the modified posture fixation cushion was used to keep the subjects in the same position for multiple scans, and the setup error was measured. After the virtual 3D image was automatically adapted to the real spine, the registration error was also measured. Only when the setup error and registration error are within a relatively acceptable range can MRsp technology be well applied to clinical patients for lumbar puncture. This was the first time MR technology was applied in the field of spinal puncture for humans. Another difference between the studies was the headset used. Sargsyan used the Meta 2 Headset by Metavision, while HoloLens 2 by Microsoft was used in the present study. The Meta 2 headset has some advantages, such as price and a larger field of view (FOV) of 90°. However, as an augmented reality device, it requires a connection to a high-performance computer for its operation, which makes it heavier and less comfortable for the wearer. The HoloLens is wireless and can be used independently without the need for an external connection. It is convenient and more comfortable for users. Although the FOV of the HoloLens is 30°, it was large enough for our study.

Position consistency guarantees perfect adaptation between the virtual image and the real body. The results indicated that the average setup error in the AP direction of the CT bed was approximately 0.3 cm. The setup errors in the LR and SI directions of the CT bed were smaller, with average values of approximately 0.1 cm and 0.2 cm, respectively. Other studies reported similar setup errors in the field of radiotherapy. Hui et al measured the three-dimensional patient setup errors at different treatment sites by tomotherapy megavoltage CT and found that the average setup errors for spine sites were 4.3 mm in the lateral direction, 4.5 mm in the craniocaudal direction, and 4.1 mm in the vertical direction.<sup>28</sup> Sasaki et al set 2 mm as the criterion when studying the dosimetric impact of translational and rotational setup errors for spine stereotactic body radiotherapy.<sup>29</sup> The setup error in the present study showed acceptable consistency in the LR and SI directions of the bed between the two CT scans. Considering that the subject was in the lateral decubitus position when

undergoing the CT scans, the AP direction of the CT bed equaled the craniocaudal axis of the subject. This displacement can be adjusted by manually fine-tuning the virtual markers to match the real ones.

Currently, there are no universal standards for MR registration errors. Several studies have focused on the registration error of MR between virtual images and reality. Uhl et al evaluated the positional error of an MR-assisted technique for puncture of the common femoral artery in a phantom model and found a median axial positional error of 1.0 mm and a median sagittal positional error of 1.1 mm.<sup>30</sup> McJunkin et al demonstrated that an MR headset can be used to display interactive 3D anatomic structures of the temporal bone that can be overlaid on physical models, and the average target registration error of their system was 5.76 mm.<sup>31</sup> Gibby et al used MR technology to guide the insertion of a percutaneous pedicle screw in a lumbar spine silicone model and found that the average registration error between the virtual image and the model was 0.25 cm.<sup>32</sup> The model, with the shape of a regular hexagonal column, more easily completed the virtual-real overlap. However, the real human spine is a very complicated structure. The superimposition is more difficult than that of the regular model. In the present study, the research subjects were humans. The average registration error in the SI direction of the CT bed was only approximately 0.1 cm, which meant that the registration error along the craniocaudal axis of the human body was very small. In the AP direction of the CT bed, the average error was larger, approximately 0.3 cm. Considering that displacements of the human body in the AP direction do not affect the location of spinal puncture, the registration error in the LR direction of the CT bed was not calculated.

The average width and height of the L3-L4 intervertebral space in Chinese people are 1.31 cm and 1.12 cm, respectively.<sup>33</sup> Therefore, the registration error in this study was relatively small, approximately one-fourth the width of the interlaminar space and one-tenth the height of the interlaminar space, which lays the foundation for the future application of MRsp. With the improvement of MR technology, further randomized controlled studies will be carried out to study the success rate and incidence of complications of MRsp.

The real spine is individual and irregular, and complex structures such as the spinous process, transverse process, and articular process increase the difficulty of superimposing the virtual image on the real spine, which requires considerable time. Hence, a QR code was placed on the surface of the back skin. The code has the advantages of fast automatic processing, large information capacity, high reliability, easy recognition by HoloLens, and low cost.<sup>34</sup> The relative position between the QR code and the spine was constant both on the real body and the virtual image. As long as the virtual QR code was successfully superimposed on the real QR code, the spine could also be quickly and successfully combined. In this study, the HoloLens scanned, identified, and calculated the spatial position of the QR code to match the virtual image with the real lumbar spine in approximately one second. This fast recognition method helped to shorten the preparation time. The detailed steps are as follows:

- (a) The feature points of the QR code in the virtual image were determined in advance to be matched with the real QR code.
- (b) On the HoloLens, real-time images were obtained by the camera on the headset.
- (c) Analysis of the obtained real-time scene was conducted. The ORB (oriented FAST and rotated BRIEF) algorithm was used to find the corresponding feature points in the scene. The fast library for approximate nearest points (FLANN) algorithm was used to match the virtual QR code feature points with the real QR code.
- (d) Once the virtual QR code was superimposed on the real QR code, the virtual spine was also quickly superimposed on the real spine. Finally, the spatial positions of the virtual beacons were adjusted in four directions until they completely overlapped with the real beacons.

This study had several limitations. First, as each subject needed to undergo three CT scans to evaluate the setup error and the registration error in this preclinical study, it was difficult to recruit volunteers, and the sample size was only 12. However, since we have already verified that the setup error and the registration error were within the acceptable range, patients recruited for future clinical studies of MRsp will only need to undergo one CT scan preoperatively, lowering the radiation exposure significantly. Second, considering that young people have relatively few lumbar osteophytes, it was easy to find the upper and lower edges of the lumbar spinous process on CT images. We recruited young volunteers to conduct this preliminary study on the accuracy of bone image registration. Elderly patients with spinal deformities will

be more challenging and have more clinical significance. Currently, we are conducting a further randomized controlled study to compare the success rate of MRsp versus landmark-guided spinal puncture in elderly patients aged 65 or older. Third, in this preclinical study, the setup error and the registration error of MRsp were measured in the lateral decubitus position since spinal anesthesia is usually performed in the lateral decubitus position in China. Whether MRsp technology is also suitable for spinal anesthesia performed in the sitting position needs further evaluation.

## Conclusions

We developed MR-guided visualization technology for spinal puncture procedures and measured the setup and registration errors, which were found to be within the clinically acceptable range. The MRsp technology can accurately and quickly superimpose the reconstructed 3D CT images over a real human spine. To our knowledge, this is the first time MR technology has been applied in the field of spinal puncture in humans. Further randomized controlled studies should be designed in elderly patients to verify whether MRsp could improve the success rate of spinal puncture compared to conventional landmark-guided techniques.

## Data Sharing Statement

The raw data supporting the conclusions of this article will be made available by the author (Jiajun Wu, 18721754415@163.com) without undue reservation.

## Ethics Approval

The study was conducted in accordance with the Declaration of Helsinki and approved by the Institutional Review Board of Fudan University (protocol code 2023K015, 20 February 2023). This trial was registered at [chictr.org.cn](http://chictr.org.cn) (ChiCTR2300068525; <https://www.chictr.org.cn/showproj.aspx?proj=190253>; date of registration: February 2023).

## Informed Consent Statement

Informed consent was obtained from all subjects involved in the study.

## Acknowledgments

The authors would like to acknowledge Zhichao Jin (Department of Health Statistics, Second Military Medical University, Shanghai, China) for his assistance with statistical consultation.

## Author Contributions

Co-first authors: J.W. and L.G. Co-corresponding authors: W.G. and J.Q. These authors contributed equally to this work. All authors made a significant contribution to the work reported in the conception, study design, execution, acquisition of data, analysis, interpretation, or in all these areas; took part in drafting, revising, or critically reviewing the article; gave final approval of the version to be published; have agreed on the journal to which the article has been submitted; and agree to be accountable for all aspects of the work and have read and approved the final manuscript.

## Funding

This research was supported by the Project of Health and Medical Research of Shanghai (Grant No. 202240045), the Clinical Research Program of Huadong Hospital (Grant No. HDLC2022011), the Shanghai Municipal Health Commission (Grant No. 2022JC025), the Project of Science and Technology Commission of Shanghai Municipality (20Y11900200), the Natural Science Foundation of Tibet Autonomous Region (Grant No. XZ2022ZR-ZY26(Z)), the National Key R&D Program of China (2018YFC2002000), the High-level Local University Construction Project of Shanghai Medical College (FNDGJ202212) and the Fund of Shanghai Municipal Education Commission (C2023244).

## Disclosure

The authors declare no conflicts of interest in this work.

## References

1. Liu B, Liu S, Wang Y, et al. Enhanced recovery after intraspinal tumor surgery: a single-institutional randomized controlled study. *World Neurosurg.* 2020;136:e542–e552. doi:10.1016/j.wneu.2020.01.067
2. Beverly A, Kaye AD, Ljungqvist O, Urman RD. Essential elements of multimodal analgesia in enhanced recovery after surgery (ERAS) guidelines. *Anesthesiol Clin.* 2017;35:e115–e143. doi:10.1016/j.anclin.2017.01.018
3. Grant MC, Sommer PM, He C, et al. Preserved analgesia with reduction in opioids through the use of an acute pain protocol in enhanced recovery after surgery for open hepatectomy. *Reg Anesth Pain Med.* 2017;42:451–457. doi:10.1097/AAP.0000000000000615
4. Stubbs BM, Badcock KJM, Hyams C, Rizal FE, Warren S, Francis D. A prospective study of early removal of the urethral catheter after colorectal surgery in patients having epidural analgesia as part of the Enhanced Recovery After Surgery programme. *Colorectal Dis.* 2013;15:733–736. doi:10.1111/codi.12124
5. Weiss R, Pöpping DM. Is epidural analgesia still a viable option for enhanced recovery after abdominal surgery. *Curr Opin Anaesthesiol.* 2018;31:622–629. doi:10.1097/ACO.0000000000000640
6. Osseis M, Weyrech J, Gayat E, et al. Epidural analgesia combined with a comprehensive physiotherapy program after cytoreductive surgery and HIPEC is associated with enhanced post-operative recovery and reduces intensive care unit stay: a retrospective study of 124 patients. *Eur J Surg Oncol.* 2016;42:1938–1943. doi:10.1016/j.ejso.2016.06.390
7. Niu Z, Feng W, Lyu L, Dong H, Chu H. Improvement of recovery parameters using patient-controlled epidural analgesia for video-assisted thoracoscopic surgery lobectomy in enhanced recovery after surgery: a prospective, randomized single center study. *Thorac Cancer.* 2018;9:1174–1179. doi:10.1111/1759-7714.12820
8. Brown JK, Singh K, Dumitru R, Chan E, Kim MP. The benefits of enhanced recovery after surgery programs and their application in cardiothoracic surgery. *Methodist DeBakey Cardiovasc J.* 2018;14:77–88. doi:10.14797/mdcj-14-2-77
9. Cramm SL, Luckhurst C, Galls A, et al. Thoracic epidural-based Enhanced Recovery After Surgery (ERAS) pathway for Nuss repair of pectus excavatum shortened length of stay and decreased rescue intravenous opiate use. *Pediatr Surg Int.* 2021;37:1191–1199. doi:10.1007/s00383-021-04934-x
10. Harbaugh CM, Johnson KN, Kein CE, et al. Comparing outcomes with thoracic epidural and intercostal nerve cryoablation after Nuss procedure. *J Surg Res.* 2018;231:217–223. doi:10.1016/j.jss.2018.05.048
11. Duniec L, Nowakowski P, Kosson D, Łazowski T. Anatomical landmarks-based assessment of intravertebral space level for lumbar puncture is misleading in more than 30%. *Anesthesiol Intensive Ther.* 2013;45:1–6. doi:10.5603/AIT.2013.0001
12. Oliveira de Filho GR, Gomes HP, da Fonseca MHZ, Hoffman JC, Pederneiras SG, Garcia JHS. Predictors of successful neuraxial block: a prospective study. *Eur J Anaesthesiol.* 2002;19:447–451. doi:10.1017/S0265021502000716
13. Qureshi AI, Khan AA, Malik AA, et al. Lumbar catheter placement using paramedian approach under fluoroscopic guidance. *J Vasc Interv Neurol.* 2016;8:55–62.
14. Belavy D, Ruitenbergh MJ, Brijball RB. Feasibility study of real-time three-/four-dimensional ultrasound for epidural catheter insertion. *Br J Anaesth.* 2011;107:438–445. doi:10.1093/bja/aer157
15. Hu HZ, Feng XB, Shao ZW, et al. Application and prospect of mixed reality technology in medical field. *Curr Med Sci.* 2019;39:1–6. doi:10.1007/s11596-019-1992-8
16. Smith RT, Clarke TJ, Mayer W, Cunningham A, Matthews B, Zucco JE. Mixed reality interaction and presentation techniques for medical visualisations. *Adv Exp Med Biol.* 2020;1260:123–139.
17. Parveau M, Adda M. 3iVClass: a new classification method for virtual, augmented and mixed realities. *Procedia Comp Sci.* 2018;141:263–270. doi:10.1016/j.procs.2018.10.180
18. Navarro-Martin A, Cacicedo J, Leaman O, et al. Comparative analysis of thermoplastic masks versus vacuum cushions in stereotactic body radiotherapy. *Radiat Oncol.* 2015;10:176. doi:10.1186/s13014-015-0484-7
19. Tanaka K, Irikoma S, Kokubo S. Identification of the lumbar interspinous spaces by palpation and verified by X-rays. *Braz J Anesthesiol.* 2013;63:245–248. doi:10.1016/S0034-7094(13)70224-1
20. Li M, Ni X, Xu Z, et al. Ultrasound-assisted technology versus the conventional landmark location method in spinal anesthesia for cesarean delivery in obese parturients: a randomized controlled trial. *Anesth Analg.* 2019;129:155–161. doi:10.1213/ANE.0000000000003795
21. Ye W, Zhang X, Li T, Luo C, Yang L. Mixed-reality hologram for diagnosis and surgical planning of double outlet of the right ventricle: a pilot study. *Clin Radiol.* 2021;76:237.e1–237.e7. doi:10.1016/j.crad.2020.10.017
22. Sun GC, Wang F, Chen XL, et al. Impact of virtual and augmented reality based on intraoperative MRI and functional neuronavigation in glioma surgery involving eloquent areas: a prospective controlled study. *World Neurosurg.* 2016;96:375–382. doi:10.1016/j.wneu.2016.07.107
23. Duff M, Chen Y, Cheng L, et al. Adaptive mixed reality rehabilitation improves quality of reaching movements more than traditional reaching therapy following stroke. *Neurorehabil Neural Repair.* 2013;27:306–315. doi:10.1177/1545968312465195
24. Sappenfield JW, Smith WB, Cooper LA, et al. Visualization improves supraclavicular access to the subclavian vein in a mixed reality simulator. *Anesth Analg.* 2018;127:83–89. doi:10.1213/ANE.0000000000002572
25. Wang J, Suenaga H, Hoshi K, et al. Augmented reality navigation with automatic marker-free image registration using 3-D image overlay for dental surgery. *IEEE Trans Biomed Eng.* 2014;61:1295–1304. doi:10.1109/TBME.2014.2301191
26. Sargsyan N, Bassy R, Wei X, et al. Augmented reality application to enhance training of lumbar puncture procedure: preliminary results. *CAINE.* 2019;63:189–196.
27. Freschi C, Parrini S, Dinelli N, Ferrari M, Ferrari V. Hybrid simulation using mixed reality for interventional ultrasound imaging training. *Int J Comput Assist Radiol Surg.* 2015;10:1109–1115. doi:10.1007/s11548-014-1113-x
28. Hui SK, Luszczek E, DeFor T, Dusenbery K, Levitt S. Three-dimensional patient setup errors at different treatment sites measured by the Tomotherapy megavoltage CT. *Strahlenther Onkol.* 2012;188:346–352. doi:10.1007/s00066-011-0066-z
29. Sasaki M, Nakamura M, Mukumoto N, Nakata M, Hiraoka M. Dosimetric impact of translational and rotational setup errors for spine stereotactic body radiotherapy: a phantom study. *Med Dosim.* 2018;43:320–326. doi:10.1016/j.meddos.2017.10.009
30. Uhl C, Hatzl J, Meisenbacher K, Zimmer L, Hartmann N, Böckler D. Mixed-reality-assisted puncture of the common femoral artery in a phantom model. *J Imaging.* 2022;16:47. doi:10.3390/jimaging8020047

31. McJunkin JL, Jiramongkolchai P, Chung W, et al. Development of a mixed reality platform for lateral skull base anatomy. *Otol Neurotol.* 2018;39:e1137–e1142. doi:10.1097/MAO.0000000000001995
32. Gibby JT, Swenson SA, Steve C, Rao R, Javan R. Head-mounted display augmented reality to guide pedicle screw placement utilizing computed tomography. *Int J Comput Assist Radiol Surg.* 2019;14:525–535. doi:10.1007/s11548-018-1814-7
33. Jia YT, Hou GZ, Si DW, Zhang TC, Liu XJ. Anatomical measurement and clinical significance of lumbar laminar space. *J Hebei United Univ Health Sci.* 2015;17:92–93.
34. Papaefthymiou M, Hildenbrand D, Papagiannakis G. A conformal geometric algebra code generator comparison for virtual character simulation in mixed reality. *Adv Appl Clifford Al.* 2017;27:2051–2066. doi:10.1007/s00006-016-0689-3

### Therapeutics and Clinical Risk Management

Dovepress

### Publish your work in this journal

Therapeutics and Clinical Risk Management is an international, peer-reviewed journal of clinical therapeutics and risk management, focusing on concise rapid reporting of clinical studies in all therapeutic areas, outcomes, safety, and programs for the effective, safe, and sustained use of medicines. This journal is indexed on PubMed Central, CAS, EMBase, Scopus and the Elsevier Bibliographic databases. The manuscript management system is completely online and includes a very quick and fair peer-review system, which is all easy to use. Visit <http://www.dovepress.com/testimonials.php> to read real quotes from published authors.

Submit your manuscript here: <https://www.dovepress.com/therapeutics-and-clinical-risk-management-journal>